Tunable Topological Floquet Bound States in the Continuum in a Periodically Driven Double SSH Chain

Xian Duan(段显)[1], Ruozhen Wang(王若圳)[1], Bo Zhu(朱博)[1*], Zhi Tan(谭智)[1,2*], Honghua Zhong(钟宏华)[1,3*], and Shu Chen(陈澍)[4]

[1]*School of Electronic Information and Physics, Central South University of Forestry and Technology, Changsha 410004, China*
[2]*Institute of Quantum Precision Measurement, State Key Laboratory of Radio Frequency Heterogeneous Integration, College of Physics and Optoelectronic Engineering, Shenzhen University, Shenzhen 518060, China*
[3]*Key Laboratory of Low-Dimension Quantum Structures and Quantum Control of Ministry of Education, Synergetic Innovation Center for Quantum Effects and Applications, and Department of Physics, Hunan Normal University, Changsha 410081, China*
[4]*Beijing National Laboratory for Condensed Matter Physics, Institute of Physics, Chinese Academy of Sciences, Beijing 100190, China*

(Received 20 May 2025; accepted manuscript online 10 July 2025)

We propose a novel approach to generate and manipulate topological Floquet bound states in the continuum (BICs) via a class of systems constructed by coupling two identical periodically driven one-dimensional Su–Schrieffer–Heeger chains. The formation of topological Floquet BICs can be adjusted only by tuning the driving amplitude or frequency, regardless of whether the static system has BICs or not. The interchain bias can only change the localization property of topological Floquet BICs, and a bigger bias can lead to transforming topological Floquet BICs into bound states out of the continuum (BOCs). But it does not change the topological properties of these topological Floquet states. Based on the repulsion effect of edge states, we propose to detect occurrence of topological Floquet BICs and transition point between topological Floquet BICs and BOCs using quantum walk. Our work provided a convenient and realistic approach for the experimental realization and manipulation of BICs in a single-particle quantum system.

DOI: 10.1088/0256-307X/42/9/090601 CSTR: 32039.14.0256-307X.42.9.090601

1. Introduction. Topological bound states in the continuum (BICs), topologically protected localized interface modes whose energies are embedded in the continuous spectrum of extended states, have attracted much attention in several physical fields ranging from condensed-matter physics to optics.[1–15] Their unique properties have led to numerous applications, including lasers, sensors, and beam shaping.[16,17] Topological BICs are generally robust against local perturbations when the number of parameters one can tune equals the number of equations required to satisfy the topological BICs condition; thus, they can exist in only a few special systems. Recently, theoretical works have suggested topological BICs in a two-dimensional (2D) lattice,[4–6] as observed in a variety of synthetic photonic structures that allow robust control of parameters.[8,9,18] These types of topological BICs manifest themselves through corner states achieved by engineering the potential or the hopping rate. Therefore, such previous studies have been limited to considering static (i.e., undriven) lattices. In particular, the realization of topological BICs in quantum systems still remains a challenge.

Floquet BICs were recently suggested in periodically driven Floquet systems, which can appear in the bulk[19–22] or at the edges of finite lattices.[23,24] It has been shown that the resonant interplay between the periodic driving and tilt may lead to a virtual surface defect in the defect-free semilattice, thus resulting in Floquet-surface BICs.[24] However, these states are nontopological. Although a recent work reported topological Floquet BICs[25] existing in a complex helical waveguide 2D array with a refractive index gradient and zigzag-zigzag edges, the refractive index gradient plays a key role in forming topological Floquet BICs; otherwise, no topological Floquet BICs are observed without a refractive index gradient. Thus, the natural question to consider is: can topological Floquet BICs be realized using a simple quasi-1D defect-free lattice? If so, what is the effect of the gradient field? How can we manipulate these topological Floquet BICs via the driving field? Finding such an easily generalizable design route for topological Floquet BICs is undoubtedly of great significance.

In this study, we show that topological Floquet BICs appear in a periodically driven double Su–Schrieffer–Heeger (SSH) chain. In such systems, the block-diagonalization can separate the Hilbert space into a

*Corresponding authors. Email: zhubo163ky@163.com; 2350453001@email.szu.edu.cn; hhzhong115@163.com
© 2025 Chinese Physical Society and IOP Publishing Ltd. All rights, including for text and data mining, AI training, and similar technologies, are reserved.

topological and a nontopological subspace. Bulk-boundary correspondence in the topological subspace guarantees the existence of a localized interface state that can lie in the continuum of extended states in the nontopological subspace, forming BICs. Especially, the formation of topological Floquet BICs can be adjusted by tuning multiple parameters, including coupling parameter θ, the driving amplitude, and frequency.

2. Generation of Topological Floquet BICs. We start by considering two directly coupled identical 1D SSH chains with external periodic driving [see Fig. 1(a)], which are described by the following Hamiltonian in the tight-binding formalism,

$$\begin{aligned} H = & \sum_n J_1[c^\dagger_{A,n}c_{B,n} + c^\dagger_{D,n}c_{C,n}] \\ & + \sum_n J_2[c^\dagger_{A,n}c_{D,n} + c^\dagger_{B,n}c_{C,n}] \\ & + \sum_n J_3[c^\dagger_{D,n}c_{A,n+1} + c^\dagger_{C,n}c_{B,n+1}] + \text{h.c.} \\ & + \sum_n \Delta[c^\dagger_{A,n}c_{A,n} - c^\dagger_{B,n}c_{B,n} \\ & - c^\dagger_{C,n}c_{C,n} + c^\dagger_{D,n}c_{D,n}]. \end{aligned} \tag{1}$$

It contains four sublattices per unit cell, where $c^{(\dagger)}_{j,n}$ with $j = A, B, C, D$ is the annihilation (creation) operator of sublattice j in the n-th unit cell ($n = 0, \pm1, \pm2, \ldots$). The interchain coupling J_1, intracell coupling J_2, and intercell coupling J_3 are

$$\begin{aligned} J_1 &= v_0(1 + \xi\cos\theta)\mathrm{e}^{-\mathrm{i}F\sin(\omega t)a_0}, \\ J_2 &= v(1 + \xi\cos\theta)\mathrm{e}^{-\mathrm{i}F\sin(\omega t)b_0}, \\ J_3 &= v(1 - \xi\cos\theta)\mathrm{e}^{-\mathrm{i}F\sin(\omega t)c_0}, \end{aligned} \tag{2}$$

where v_0 and v are the constant coupling strengths, ξ is the modulation amplitude, θ/π is a cyclical parameter varying continuously from 0 to 2, F is the driving amplitude, and ω is the driving frequency. In addition, a_0, b_0, and c_0 are lattice constants, where we set $a_0 = b_0$ and $b_0 + c_0 = 1$ is the unit. The parameter Δ represents the interchain energy bias. The Floquet topological features of this analogous model have been investigated in different physical contexts, including optical lattices [26–28] and waveguide arrays. [29–32] For simplicity, we will fix $v = 1$ as the unit and $\xi = 0.5$. In the absence of interchain coupling, namely, $v_0 = 0$, the system has two doubly degenerate Floquet SSH bands, which have quantized Zak phases as required by the existence of inversion symmetry in each chain. The presence of interchain coupling may lift the degeneracy but does not break inversion symmetry. Thus, the block-diagonalization can separate the Hilbert space into a topological and a nontopological subspace. This topological state can be used to create a topological BIC if its energy overlaps with the continuum of nontopological modes due to its symmetry protection.

According to the Floquet theorem, the evolution of a time-dependent system is governed by the one-period time-evolution operator

$$U \equiv U(T, 0) = Q \cdot \mathrm{e}^{-\mathrm{i}\int_0^T H(t)\mathrm{d}t}, \tag{3}$$

where Q denotes the time ordering. According to the evolution operator, the Floquet bands of the first Floquet Brillouin zone ($-\omega/2 \le E \le \omega/2$) are characterized by the effective Hamiltonian $H_{\text{eff}} = \mathrm{i}\ln U/T$. Then the quasienergy of the system E can be obtained by diagonalizing the effective Hamiltonian H_{eff}. The search for bound states, either embedded or outside the spectrum of scattered states, is done by inspecting the inverse participation ratio (IPR) when the quasienergies and their corresponding eigenvectors are determined. For the mth quasienergy eigenstate $\psi(E_m)$, $1 \le m \le N$, which is spanned as $\psi(E_m) = \sum_j \sum_n a^m_n |n, j\rangle$ in the single-particle Hilbert space, the IPR is defined as [24]

$$\text{IPR}(E_m) = \frac{\sum_n |a^m_n|^4}{(\sum_n |a^m_n|^2)^2}. \tag{4}$$

Then, the IPR of the localized (bound) state has nonzero values, while the extended (scattered) state tends to zero for large N.

To show topological Floquet BICs generated by the periodically driven double SSH chain, we consider the energy spectrum and corresponding IPR under different coupling strengths. In Figs. 1(b)–1(e), we first show the case of

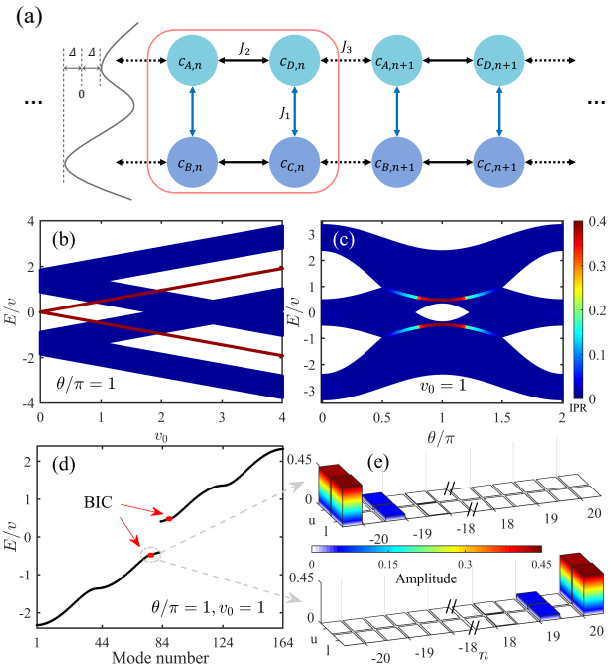

Fig. 1. (a) Schematic diagram of the double SSH chain. The solid red box shows a unit cell, A, B, C, and D denote the sublattices in a cell, J_1 is the interchain coupling, while J_2 and J_3 are intracellular and intercellular couplings, respectively, and Δ is the energy bias between two chains. (b) Quasienergy E/v versus the interchain coupling v_0 for $\theta/\pi = 1$. (c) Quasienergy E/v versus the modulated coupling parameter θ/π for $v_0 = 1$. The depth of color indicates the corresponding inverse participation ratio of energy. (d) The topological interface mode is inside the continuum, and the topological Floquet BICs are indicated by the red dots. (e) The density distribution of a pair of degenerate topological Floquet BICs; u and l represent the indicators of the upper and lower chain, respectively. The other parameters are chosen as $\Delta = 0$, $F = 1$, $\omega = 20$, $a_0 = b_0 = 0.4$, $c_0 = 0.6$, and the total unit cell $N = 41$.

a symmetric double SSH chain with $\Delta = 0$. An inspection of the quasienergy diagram shows that pairwise edge states can move continuously into and out of the bulk continuum by tuning the interchain coupling v_0, which indicates that Floquet BICs emerge in pairs for $0.8 < v_0 < 2$ [see Fig. 1(b)]. In addition, for a fixed interchain coupling $v_0 = 1$, as the coupling modulation changes to $0.5 < \theta/\pi < 1.5$, Floquet BICs also emerge in pairs [see Fig. 1(c)], which are clearly visible in the eigenenergy spectrum diagram [see Fig. 1(d)]. Interestingly, by inspecting the corresponding density distribution of Floquet BICs for the parameter $\theta/\pi = 1$, it is found that these Floquet BICs are doubly degenerate edge states due to the inversion symmetry along the transverse direction, which are symmetrically localized at two left or right edge sites of the double SSH chain [see Fig. 1(e)]. The topological property of these Floquet BICs can be characterized by the Zak phase [see Supplementary Materials (SM)]; they are topologically protected [see Fig. 3(e)], which we call topological Floquet BICs. This explains the physical origin of topological Floquet BICs: certain interchain couplings allow the Hilbert space of the whole system to be separated into a nontopological subspace and a Floquet topological subspace via block-diagonalization, in which nontopological bands coexist with Floquet topological bands characterized by quantized Zak phases due to their symmetry protection. Therefore, these topological Floquet BICs are robust against parameter fluctuations and exist in a wide parametric region due to their topological essence (see SM).

We consider the manipulation of topological Floquet BICs via periodical driving. We consider two cases: the system initially with and without BICs. For the case of initial BICs with weak driving amplitude, the topological Floquet BICs can remain in the high-frequency region; however, they can become as bound states out of the continuum (BOCs) in certain low-frequency regions [see Fig. 2(a)]. The transformation between topological Floquet BICs and BOCs can alternately appear as a change in the driving parameter F/ω for high-frequency driving [see Fig. 2(b)]. Especially, for the case of the system initially without BICs, the topological Floquet BICs can reappear via a weak driving field with middle frequency, and they can remain in a wide parametric region of F/ω [see Fig. 2(c)]. The topological Floquet BICs can also reappear for high-frequency driving fields with middle driving amplitude though they exist in some narrow parametric regions [see Fig. 2(d)]. Therefore, whethers or not the static system has BICs, the formation of topological Floquet BICs can be realized only by tuning the driving amplitude or frequency.

Now, we discuss the effect of interchain bias on the properties of topological Floquet BICs. Due to nonzero bias Δ, two chains are no longer equivalent, so the inversion symmetry along the longitudinal direction is broken. In Fig. 3(a), we show the energy spectrum versus the strength of bias Δ. Obviously, the IPR of topological Floquet BICs rises as the strength of bias increases,

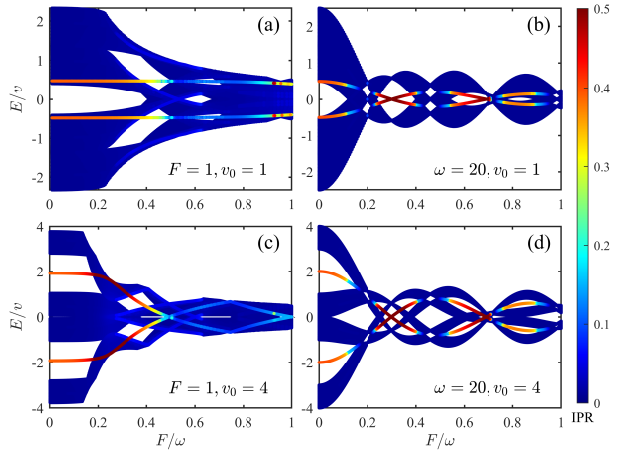

Fig. 2. Quasienergy E/v versus the driving parameter F/ω for different interchain coupling strengths $v_0 = 1$ (original BICs) and $v_0 = 4$ (original BOCs), respectively. (a) and (c) The variable quantity is the driving frequency for fixed $F = 1$. (b) and (d) The variable quantity is the driving amplitude for fixed $\omega = 20$. The other parameters are chosen as $\theta/\pi = 1$, $\Delta = 0$, and $N = 41$.

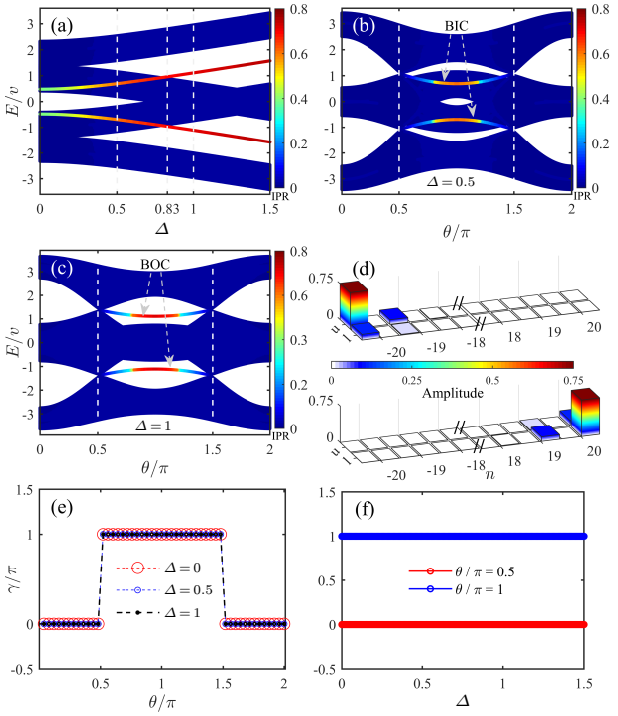

Fig. 3. (a) Quasienergy E/v versus the strength of bias Δ for $\theta/\pi = 1$. (b) and (c) Quasienergy E/v versus the coupling modulation parameter θ/π for $\Delta = 0.5$ and $\Delta = 1$, respectively. (d) The density distribution of a pair of topological Floquet BICs for $\Delta = 0.5$. (e) The Zak phase versus the coupled modulated parameter θ/π for $\Delta = 0$ (red circle dotted line), $\Delta = 0.5$ (blue circle dotted line), and $\Delta = 1$ (black circle dotted line). (f) The Zak phase versus the strength of bias Δ. The other parameter are chosen as $v_0 = 1$, $F = 1$, $\omega = 20$, and $N = 41$.

which means the density distribution of topological Floquet BICs becomes more localized and that topological Floquet BICs become BOCs when $\Delta > 0.83$. The larger bias can induce a division between bulk bands and af-

fect their position in the continuum of topological Floquet BICs [see Figs. 3(b) and 3(c)]. Different from the system without bias, doubly degenerate topological Floquet BICs are asymmetrically localized at two left or right edge sites of a double SSH chain, as shown in Fig. 3(d). It is worth noting that the bias only can change the localization property of topological Floquet BICs and does not change their topological properties [see Figs. 3(e) and 3(f)]. Our results may provide a new way to prepare and manipulate topological Floquet BICs.

3. Dynamical Detection. The repulsion effect of edge states may provide a promising approach for experimentally detecting the topological Floquet BICs (see SM). In experiments, one can detect the long-time average of the edge degree,

$$D_{\mathrm{u(l)}} = \frac{1}{T'}\sum_{n}\int_{0}^{T'} |n| P_{n}^{\mathrm{u(l)}}(t)\mathrm{d}t, \tag{5}$$

where $P_{n}^{\mathrm{u(l)}}(t) = |a_{n}^{\mathrm{u(l)},j}(t)|^2$ denotes the probability distribution of the upper (lower) chain of the double SSH chain, and T' is the total evolution time. Then the total edge degree of the system is written as $D = D_{\mathrm{u}} + D_{\mathrm{l}}$, and a larger D means more distribution in the edge sites in the long-time average. In Fig. 4(a), we show the value of D as a function of the coupling modulation parameter θ/π by selecting $T' = 400$. Obviously, due to the repulsion effect, the value of D apace decreases with the appearance of topological Floquet BICs. In addition, we also considered the influence of bias strength on edge degree. One can see that as Δ increases, the total edge degree of the system slightly increase; in this case, while increasing for upper chain's edge degree and decreasing for lower chain's edge degree, as shown in Fig. 4(b). However, when $\Delta > 0.83$, which is considered to be a transition point where topological Floquet BICs transform into topological Floquet BOCs, the value of D decreases rapidly. The primary cause is resonance between topological Floquet BICs and bulk states with energies similar to those of topological Floquet BICs. It is found that due to the energy of topological Floquet BICs residing within bulk state, as the increase of the bias Δ, the energies of topological Floquet BICs slowly approach energy of bulk state near edge, this may induce resonance effect and increase the edge degrees. However, when $\Delta > 0.83$, energies of topological Floquet BICs deviate from bulk and become topological Floquet BOCs; thus leading to rapid decrease in edge degree [see Figs. 4(b) and 3(a)]. Therefore, this may provide a feasible method for detecting occurrence of topological Floquet BICs and transition between topological Floquet BICs and BOCs.

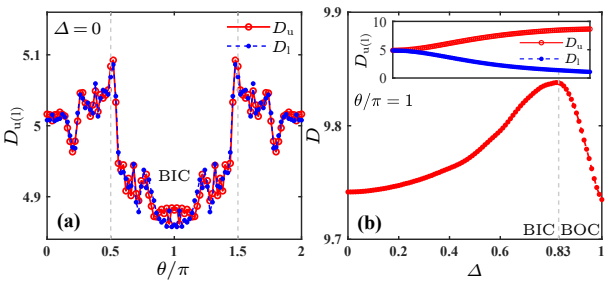

Fig. 4. Long-time average of edge degree as a function of (a) the coupling modulation parameter θ/π and (b) the bias Δ. $D_{\mathrm{u(l)}}$ denote long-time average of edge degree of upper (lower) chain. The other parameter are chosen as $v_0 = 1$, $F = 1$, $\omega = 20$, and $N = 41$.

4. Experimental Proposal. Now, we discuss the experimental possibility of observing our theoretical predictions. It is possible to realize our model via synthetic photonic [33,34] and acoustic structures. [9] Here, to propose a promising scheme for realizing BICs in quantum systems, we mainly focus on its experimental realization in quantum systems, such as cold atoms in optical lattice. Our model can be realized via quasi-1D dimerized lattices including Hubbard ladders or two coupled SSH chains. We first load ultracold atoms in a double-well superlattice potential, $V(x,y) = V_x \sin^2(\kappa x) + V_{y1}\sin^2(\kappa y) + V_{y2}\sin^2(2\kappa y + \varphi) + (V_x + V_{y1})\xi\cos\theta\sin(\kappa x)\sin(\kappa y) - V_{y2}\xi\cos\theta\sin(2\kappa x)\sin(2\kappa y)$, where V_x and $V_{y1,2}$ are the potential depths in the x and y directions; ξ and θ are the amplitude and angle of polarization respectively, which can be well controlled in real experiments; κ is the wave vector of the laser. For $V_{y1,2} \gg V_x$, there is a large tunneling barrier between double wells in the y direction; thus, low-energy physics 2D systems decouple into an array of dynamically isolated two-leg ladders with each ladder extending in the x direction. We assume that the frequency difference of lasers does not induce visible differences in wavelengths and that lattice spacing with the same frequency is approximately the same. The relative well depth of the two legs is controlled by phase φ. Staggered tunneling can also naturally arise in double-well optical lattices already engineered experimentally by increasing laser strength [35,36] or through laser-induced tunneling. [37,38] Then we adiabatically add periodic circular driving on the double-well superlattice with forms: $x \to x + f\cos(\omega t)$ and $y \to y + f\cos(\omega t)$ where f and ω denote the driving amplitude and frequency respectively. For such periodically driven two-leg SSH chains, topological Floquet BICs can be constructed by adjusting either driving amplitude or frequency regardless of whether or not BICs initially exist within this system. In addition, bosonic version of SSH model has been experimentally realized using Rydberg atoms trapped in a 1D array of optical tweezers. [39,40] Our model can also be experimentally realized via coupling these two SSH chains.

5. Summary. In summary, we have investigated construction of topological Floquet BICs by a periodically driven double SSH chain. It is found that the topological Floquet BICs can be constructed in such a system only by adjusting the driving amplitude or frequency, regardless of whether the static system has BICs or not. The interchain bias can only change the localization property of topological Floquet BICs, and a larger bias can lead to the transformation of topological Floquet BICs into BOCs. However, it does not change the topological properties of these topological Floquet states. We also provide a feasible approach for experimentally detecting the occurrence of topological Floquet BICs and the transition point between topological Floquet BICs and BOCs via quantum walk.

In addition to the discovery of topological Floquet BICs, we believe that our work brings three key advances

to related fields. First, our work may provide a convenient and realistic way for the experimental realization of BICs in a single-particle quantum system, which may accelerate the realization of quantum BICs. Second, periodic driving provides a new route to observe the transition between BICs and BOCs. Third, as the crossover between two topological Floquet BICs can be effectively controlled by adjusting periodic driving, this offers an efficient way for quantum interference involving BICs, which may promote development in applying BICs for quantum precision measurement and quantum information processing.

Acknowledgements. This work was supported by the National Natural Science Foundation of China (Grant Nos. 12175315 and 12205385).

References

[1] Zhen B, Hsu C W, Lu L, Stone A D, and Soljačić M 2014 *Phys. Rev. Lett.* **113** 257401
[2] Mukherjee S, Gomis-Bresco J, Pujol-Closa P, Artigas D, and Torner L 2018 *Phys. Rev. A* **98** 063826
[3] Bulgakov E N and Maksimov D N 2017 *Phys. Rev. Lett.* **118** 267401
[4] Yoda T and Notomi M 2020 *Phys. Rev. Lett.* **125** 053902
[5] Chen Z G, Xu C, Al Jahdali R, Mei J, and Wu Y 2019 *Phys. Rev. B* **100** 075120
[6] Benalcazar W A and Cerjan A 2020 *Phys. Rev. B* **101** 161116
[7] Cerjan A, Jürgensen M, Benalcazar W A, Mukherjee S, and Rechtsman M C 2020 *Phys. Rev. Lett.* **125** 213901
[8] Wang Y, Xie B Y, Lu Y H, Chang Y J, Wang H F, Gao J, Jiao Z Q, Feng Z, Xu X Y, Mei F, Jia S, Lu M H, and Jin X M 2021 *Light Sci. Appl.* **10** 173
[9] Xiao Y X, Ma G, Zhang Z Q, and Chan C T 2017 *Phys. Rev. Lett.* **118** 166803
[10] Liu L, Li T, Zhang Q, Xiao M, and Qiu C 2023 *Phys. Rev. Lett.* **130** 106301
[11] Hsu C W, Zhen B, Stone A D, Joannopoulos J D, and Soljačić M 2016 *Nat. Rev. Mater.* **1** 16048
[12] Koshelev K, Bogdanov A, and Kivshar Y 2019 *Sci. Bull.* **64** 836
[13] Bezus E A, Bykov D A, and Doskolovich L L 2018 *Photon. Res.* **6** 1084
[14] Guo Z W, Jiang J, Jiang H T, Ren J, and Chen H 2021 *Phys. Rev. Research* **3** 013122
[15] Song Q, Dai S, Han D, Zhang Z Q, Chan C T, and Zi J 2021 *Chin. Phys. Lett.* **38** 084203
[16] Azzam S I and Kildishev A V 2021 *Adv. Opt. Mater.* **9** 2001469
[17] Kang M, Liu T, Chan C T, and Xiao M 2023 *Nat. Rev. Phys.* **5** 659
[18] Hu Z, Bongiovanni D, Jukić D, Jajtić E, Xia S, Song D, Xu J, Morandotti R, Buljan H, and Chen Z 2021 *Light Sci. Appl.* **10** 164
[19] González-Santander C, Orellana P A, and Domínguez-Adame F 2013 *EPL* **102** 17012
[20] Longhi S and Valle G D 2013 *Sci. Rep.* **3** 2219
[21] Agarwala A and Sen D 2017 *Phys. Rev. B* **96** 104309
[22] Zhong H, Zhou Z, Zhu B, Ke Y, and Lee C 2017 *Chin. Phys. Lett.* **34** 070304
[23] Della Valle G and Longhi S 2014 *Phys. Rev. B* **89** 115118
[24] Zhu B, Ke Y G, Liu W J, Zhou Z, and Zhong H H 2020 *Phys. Rev. A* **102** 023303
[25] Li C, Kartashov Y V, and Konotop V V 2022 *Opt. Lett.* **47** 5160
[26] Li X P, Zhao E, and Liu W V 2013 *Nat. Commun.* **4** 1523
[27] Huang B, Wu Y H, and Liu W V 2018 *Phys. Rev. Lett.* **120** 110603
[28] Kang J H, Han J H, and Shin Y 2020 *New J. Phys.* **22** 013023
[29] Jangjan M and Hosseini M V 2020 *Sci. Rep.* **10** 14256
[30] Zhou L and Du Q 2020 *Phys. Rev. A* **101** 033607
[31] Padavić K, Hegde S S, DeGottardi W, and Vishveshwara S 2018 *Phys. Rev. B* **98** 024205
[32] Li C, Lin S, Zhang G, and Song Z 2017 *Phys. Rev. B* **96** 125418
[33] Vicencio R A, Cantillano C, Morales-Inostroza L, Real B, Mejía-Cortés C, Weimann S, Szameit A, and Molina M I 2015 *Phys. Rev. Lett.* **114** 245503
[34] Mukherjee S, Spracklen A, Choudhury D, Goldman N, Öhberg P, Andersson E, and Thomson R R 2015 *Phys. Rev. Lett.* **114** 245504
[35] Wirth G, Ölschläger M, and Hemmerich A 2011 *Nat. Phys.* **7** 147
[36] Sompet P, Hirthe S, Bourgund D, Chalopin T, Bibo J, Koepsell J, Bojović P, Verresen R, Pollmann F, Salomon G, Gross C, Hilker T A, and Bloch I 2022 *Nature* **606** 484
[37] Atala M, Aidelsburger M, Lohse M, Barreiro J T, Paredes B, and Bloch I 2014 *Nat. Phys.* **10** 588
[38] Philipp H, Olivier T, Alessio C, Christoph Ö, Juliette S, Julian S, Malte W, Patrick W, Klaus S, Maciej L, and André E 2012 *Phys. Rev. Lett.* **109** 145301
[39] Lienhard V, de Léséleuc S, Scholl P, Barredo D, Lahaye T and Browaeys A 2019 *Quantum Inf. Measure. (QIM) V* F4B.2
[40] de Léséleuc S, Lienhard V, Scholl P, Barredo D, Weber S, Lang N, Büchler H P, Lahaye T, and Browaeys A 2019 *Science* **365** 775